RSC Advances

This is an *Accepted Manuscript*, which has been through the Royal Society of Chemistry peer review process and has been accepted for publication.

Accepted Manuscripts are published online shortly after acceptance, before technical editing, formatting and proof reading. Using this free service, authors can make their results available to the community, in citable form, before we publish the edited article. This *Accepted Manuscript* will be replaced by the edited, formatted and paginated article as soon as this is available.

You can find more information about *Accepted Manuscripts* in the Information for Authors.

Please note that technical editing may introduce minor changes to the text and/or graphics, which may alter content. The journal's standard Terms & Conditions and the Ethical guidelines still apply. In no event shall the Royal Society of Chemistry be held responsible for any errors or omissions in this *Accepted Manuscript* or any consequences arising from the use of any information it contains.

ROYAL SOCIETY OF CHEMISTRY

www.rsc.org/advances

Synergetic photocatalysts coupling both high adsorption capacity and photocatalytic activity are prepared from highly expanded graphene oxide frameworks that are pillared by Ti-O clusters

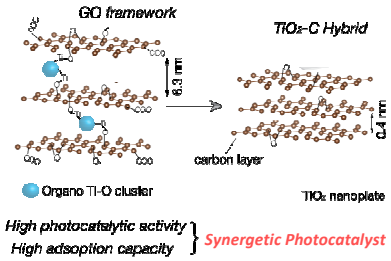

RSC Advances Accepted Manuscript

Cite this: DOI: 10.1039/c0xx00000x

www.rsc.org/xxxxxx

Communication

Synergetic photocatalysts derived from porous organo Ti-O clusters pillared graphene oxide frameworks (GOFs)

Jianbo Liang,[a] Zheng-Ming, Wang,[*a] Ming-Chao Sun [a], Noriko, Yoshizawa[b] and Hiroyuki, Kawashima[c]

Received (in XXX, XXX) Xth XXXXXXXXX 20XX, Accepted Xth XXXXXXXXX 20XX

DOI: 10.1039/b000000x

Unique nanocomposites comprising thin TiO_2 nanoplates and lamellar carbon sheets were derived from organo Ti-O clusters pillared graphene oxide (GO), a porous layered framework synthesized by intercalating GO layers with organo-Ti reagents via a simultaneous intercalation and hydrolysis process. The nanocomposites display both high adsorption capacity and enhanced photocatalytic activity towards methyl orange (MO), promising as synergetic photocatalysts for the removal of organic contaminates in water environment.

Nanocomposites that incorporate two or several parts of components into a functional integrity are attractive for the synergetic effects generated at the interface, which provide a wealth of opportunities for exploring enhanced or even new properties as well as multi-functionalities.[1-6] Optimizing each component in terms of its size, morphology and crystallinity, particularly, coupling these components by engineering the interfacial regions, are important to explore advanced materials with desired electronic, optical, mechanical, and catalytic properties.[1,3] Recent interest has been drawn to the assembly of inorganic nanocrystals with two-dimensional carbon sheets, typically, the graphene, a newly emerging two-dimensional allotrope of carbon consisting of a single atomic layer. The unique electrical conductivity and gigantic two-dimensional surface of carbon sheets can promote the charge transferring between the inorganic components, producing synergetic effects that are beneficial for enhancing the performance of photocatalysts or photodetective devices.[5, 6]

Graphene oxide (GO), a none-stoichiometric oxidized derivative of graphene containing abundant functional groups such as hydroxyl, carboxyl and epoxide groups, can display flexible intercalation behaviours.[7] Recently, a new kind of graphene oxide frameworks (GOFs) has been synthesized. Similar to the formation of covalent organic frameworks (COFs), the good reactivity of borinic acid to hydroxyl group promotes its intercalation into the GO layers, forming new porous materials potential for gas storage application.[8] We are here motivated to screen from the organo-metal reagent family, which displays good reactivity to water and hydroxyl group, to design a new type

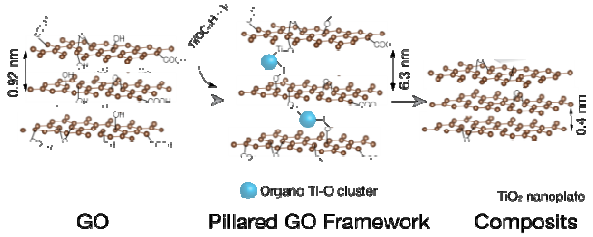

Scheme 1. Illustration of the synthesis strategy.

of GOF compounds.[9] In this study, we report a highly expanded GOF compound formed *via* intercalation of organo-Ti reagent into GO accompanied by an intra-gallery hydrolysis process. Such new GOFs can be transformed into nanocomposites of TiO_2 and lamellar carbon sheets under controlled conditions, which are promising as synergetic photocatalysts towards the treating of trace organic contaminates in water environment.

The strategy of this study is illustrated in Scheme 1. Initially, highly hydrated GO was prepared from graphite powder by the modified Hummer's method.[10, 11] GO powder was ultrasonically dispersed into anhydrous ethanol. The dispersion was then added dropwise into another transparent ethanol solution containing organo-Ti reagent (here, titanium butoxide, $Ti(OBu^n)_4$, was used to exemplify the strategy). The mixture was stirred, and heated at 65 °C for 5 hours. This aging procedure promotes the insertion of neutral $Ti(OBu^n)_4$ into the GO gallery, hereafter reacting with the inter-gallery water molecules and functional groups to form a GO intercalate. The product, identified as organo Ti-O GOF hereinafter, was recovered by centrifugation, washed by anhydrous ethanol for several times, and finally dried at 60 °C in an oven. To prepare the synergetic photocatalyst, as-prepared GO intercalate was re-dispersed in ethanol. After addition of a small amount of water or HF solution, the mixture was sealed into a Teflon-lined autoclave, and then subjected to solvothermal treatment at 180°C for 24 hours. Such a treatment will promote the removal of a major portion of functional groups, and the restoration of some aromatic linkage to form a reduced GO (rGO) layer. At the same time, the pillared GOF structure is destructed, but nonetheless the intercalated Ti species are transformed to larger TiO_2 structure and heterogeneously crystallize on the surface of rGO layers to form a nanocomposite.

RSC Advances Accepted Manuscript

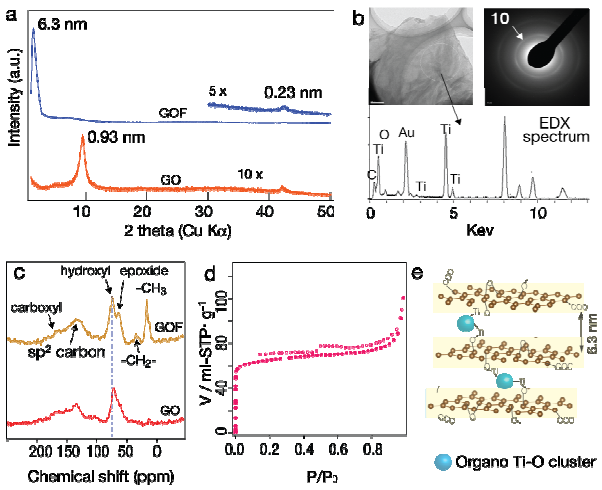

Fig1. XRD patterns (a), TEM image with SAED pattern and EDX spectrum (b), solid state ^{13}C-NMR (c), N_2 adsorption-desorption isotherm (d), and a proposed structure model of the organo Ti-O cluster pillared GOF (e). All data are those of the organo Ti-O GOF except for the bottom lines in (a) and (c) representing those of GO.

Figure 1a shows the X-ray diffraction (XRD) pattern of the GO sample. The basal spacing of 0.93 nm indicates that the sample is highly hydrated. The water content determined from thermogravimetric (TG) analysis is 14.8% (see supporting Information). The chemical formula based on elemental and TG analyses is $C_4O_{2.45}H_{1.37}$ $(H_2O)_{0.93}$. The high oxygen content may be due to a deep oxidation which generates a rich amount of functional groups. After reaction with Ti(OBu^n)$_4$, the basal peak of GO phase is thoroughly disappeared. The product displays an intensive diffraction peak corresponding to a spacing of 6.3 nm and a weak diffraction very close to the intra-layer (100) diffraction of GO, suggesting the retention of aromatic-like carbonic layers and the expansion of the gallery *via* a topotactic process. Since the basal spacing is much higher than that of ethanol-solvated GO derivatives (in a range of 1.3~1.5 nm)[12], the highly expanded 6.3 nm-phase should not arouse from the swelling of GO in ethanol, but is attributable to the intercalation of organo-Ti species within the GO gallery. TEM image (Figure 1b) shows that the sample consists of folded thin flakers. Corresponding selected area electron diffraction (SAED) pattern shows diffraction rings that can be assigned to the in-plane diffractions of GO, indicating that the host layers are randomly stacked in high disorder. Energy-dispersive X-ray (EDX) analysis reveals the presence of elements of Ti and O along with C. TG and XRD measurements show that the content of Ti-related species, if estimated as the weight of TiO_2 (the residue after TG measurement in air, see Supporting Information), is about 23.5%.

Figure 1c shows the solid state ^{13}C-nuclear magnetic resonance (NMR) spectra of the GO sample and the intercalated product. For GO, the chemical shift of 72 ppm and a shoulder at 65 ppm represent the hydroxyl and epoxide groups, respectively. The signal at 136 ppm is correlated to the aromatic sp^2 carbons located in the GO layers. Another peak at 166 ppm can be attributed to the carbonyl group.[13] After reaction with Ti(OBu^n)$_4$, two new signals located at 17 and 35 ppm appear in the spectra, which can be assigned to the –CH_3 and -CH_2- groups respectively, strongly supporting the presence of organo species. Importantly, compared with GO, the signal corresponding to the hydroxyl group (75 ppm) is apparently left-shifted. This change indicates that the intercalates strongly interact with the hydroxyl groups on the basal planes of GO layer. Considering the basal spacing of 6.3 nm, much larger than the size of Ti(OBu^n)$_4$, and the good reactivity of organo-Ti reagent towards water and hydroxyl groups, the intercalates are attributed to the organo Ti-O clusters formed from partial hydrolysis of organo-Ti reagents.[14] Presumably, the clusters are bonded with GO layers *via* a Ti-O linkage, forming a highly expanded pillared framework analogous to the GOF architectures, as proposed in Figure 1e. N_2 adsorption-desorption isotherm of this sample shows a typical shape of type I partially hybridized with type IV with medium and low pressure hysteresis branches (Figure 1d), indicative of a complex intra-gallery pore structure containing both mesopores and small size micropores. The specific surface area calculated from Brunauer-Emmett-Teller (BET) equation is 225 $m^2 \cdot g^{-1}$, supporting the porous feature of this new GOF compound.

Like compounds of metal-organic frameworks (MOFs), the organo Ti-O GOF can be facially transformed into TiO_2/carbon nanocomposites.[15] A solvothermal reaction in neutral condition is employed to remove the functional groups on GO layers, and at the same time promote the transformation of intercalated organo Ti-O clusters into well crystallized TiO_2 nanocrystallites.[14] As shown in Figure 2a, the reaction product displays diffraction patterns from both anatase-type TiO_2 (tetragonal phase, a = 0.3795(2) nm, c = 9.5156(3) nm) and in-plane structures of graphene or reduced GO layers. The content of the TiO_2 component, determined from TG data, is 54.6% (Figure 2b). ^{13}C-NMR spectra show a prominent signal corresponding to sp^2 carbons and a weak signal of epoxide group (see supporting Information), indicating that a major part of functional groups are removed, and some of aromatic carbon linkages are restored. N_2 adsorption result gives a specific surface area of 294 $m^2 \cdot g^{-1}$, which is slightly greater than that of the precursor. TEM image (Figure 2c) shows that the sample comprises micro-meter size carbon sheets, on which platelet-like and some of quasi-spherical TiO_2 nanocrystals are loaded. The lateral size of the nanoplatelet is below 30 nm. The well-developed edges indicate that the

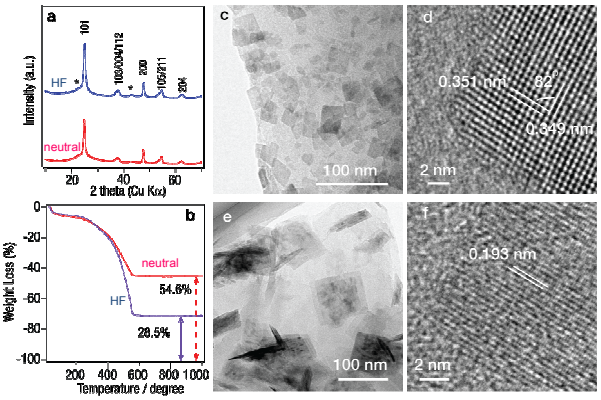

Fig2. XRD patterns (a), TG curves (b), TEM and HRTEM images of the TiO_2/ layered carbon composites prepared at neutral (c, d) and acidic condition (e, f). Asterisk marks the peak from carbon.

RSC Advances Accepted Manuscript

This journal is © The Royal Society of Chemistry [year]

nanoplatelets are highly crystallized. High resolution TEM (HRTEM) image (Figure 2d) recorded along the <111> axis shows two sets of lattice fringe. The periodic distance of 0.35(1) nm and 0.34(9) nm correlate to the (101) and (011) lattices, respectively. The cross angle between this two set fringes are measured as 82º, consistent with the theoretical value. The thickness of the nanoplatelets estimated from some vertically stacked platelets is only 3-5 nm. On the other hand, when HF is added in the solvothermal solution, the size of the TiO_2 nanoplatelets in the obtained product can reach 80 nm (Figure 2a, e). The platelets are rather thin and tend to stack in a face-to-face manner on carbon sheets. HRTEM image recorded from the <001> axis (Figure 2f) exhibits a lattice fringe around 0.193 nm, which corresponds to the inter-distance between the (100) planes. TG data shows that the weight ratio of TiO_2 is decreased to about 28.5% (Figure 2b), and is further lowered to 8.8% if 25% excessive amount HF is employed. Besides the role of selective adsorption on certain surface facets of tetragonal TiO_2 to promote anisotropic growth,[16] HF also contribute to the dissolution of a portion of organo Ti-O clusters, consequently reduce the TiO_2 content in the composite.

The TiO_2/layered carbon composites are evaluated from their adsorption and photocatalytic degradation properties towards methyl orange (MO). Compared with the commercial TiO_2 (Degussa (Evonic), P-25), the composites can rapidly adsorb MO, and the specific adsorption capacity, are much higher than that of the Degussa, P-25. The composite prepared in acidic condition shows a higher adsorption capacity than that in a neutral condition, which is mainly owing to its greater specific surface area (375 $m^2 \cdot g^{-1}$). The samples display high activity in decomposing MO under ultraviolet irradiation. The apparent rate

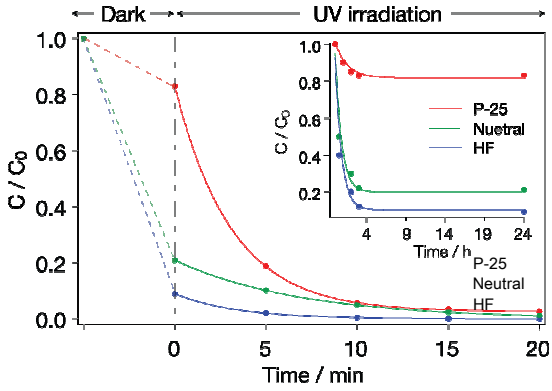

Fig3. Adsorption and photocatalytic decomposition of MO by P-25 and TiO_2/layered carbon nanocomposites prepared at neutral and acidic conditions. The inset is the adsorption results in the dark.

constants are calculated based on the 1st order kinetics (see supporting Information). Though the rate constants for the two composites are slightly lower than (neutral condition, 0.142 min^{-1}) or comparable to (acidic condition, 0.288 min^{-1}) that of P-25 (0.269 min^{-1}), if taking the content of TiO_2 into account, the composites can display a higher activity in the photodecomposition of MO as compared to the pure P-25 and other reported composites prepared by simply mixing GO dispersion with Ti precursors. [17] This result suggests the presence of synergetic effect between the TiO_2 and layered carbon sheets, similar to that observed in the TiO_2-graphene composite.[5] A tentative analysis on diffuse reflectance spectra gave a band gap value of 2.8 ev and 2.6 ev for the composites prepared at neutral and acid conditions, respectively, which is smaller than that of anatase (3.2 ev). Hence, besides the role of adsorption concentration of carbon toward hydrophobic substrate molecules, the promoted charge transferring due to the carbon platelets was considered to be a key factor to the enhancement of photoactivity of the composite.[18] Since TiO_2 precursors (organo Ti-O species) are beforehand intercalated in GO layers, the current method is beneficial for achieving well dispersed TiO_2 in graphene matrix whose platelet morphologies can lead to a more sufficient contact with carbon surface and thus more efficiently improve the electron-hole charge separation as compared to other reported composites. Furthermore, the thin TiO_2 nanoplatelets themselves with preferentially exposed crystalline planes such as (001) and (111) are expected to be highly active in the photocatalysis reaction, and contribute to the high performance of the composites.[19] Considering the high adsorption capacity and the enhanced photocatalytic performance, the TiO_2/layered carbon composites derived from the organo Ti-O clusters pillared GOF compound are promising as synergetic photocatalysts for the removal of trace organic contaminates in water environment.

In summary, a new organo Ti-O cluster pillared GOF is synthesized by reaction of organo-Ti reagent with highly hydrated GO in anhydrous ethanol. The structure of this GOF compound is analysed from XRD, TEM, ED, TG, and ^{13}C-NMR data, based on which the intercalation process is proposed. We develop a facile route to transform this GOF into composites made by TiO_2 nanoplatelets and layered carbon, which show both high adsorption capacity and enhanced photocatalytic performance. Considering the large variety of organo-metal reagents, this study provides new strategy to design novel organo-metal pillared GOFs and to take advantage of the synergetic integrity properties of their functional nanocomposite derivatives.

Notes and references

[a] *Adsorption and Decomposition Research Group, Research Institute for Environmental Management Technology, National Institute of Advanced Industrial Science and Technology,1-16 Onogawa, Tsukuba, Ibaraki 305-5869, Japan. E-mail: zm-wang@aist.go.jp*
[b] *Energy Storage Materials Group, Energy Technology Research Institute, National Institute of Advanced Industrial Science and Technology,1-16 Onogawa, Tsukuba, Ibaraki 305-5869, Japan.*
[c] *Advanced Fuel Group, Energy Technology Research Institute, National Institute of Advanced Industrial Science and Technology,1-16 Onogawa, Tsukuba, Ibaraki 305-5869, Japan.*

† Electronic Supplementary Information (ESI) available: []. See DOI: 10.1039/b000000x/

1 C. Sanchez, P. Belleville, M. Popall and L. Nicole, *Chem. Soc. Rev.*, 2012,**41**, 7291-7321.
2 J. L. Shi, Chem. Rev., 2013, **113**, 2139–2181.
3 M. B. Sassin, C. N. Chervin, D. R. Rolison and J. W. Long, *Acc. Chem. Res.*, 2013, **46** , 1062–1074.
4 H. Bai, C. Li and G. Q. Shi, *Adv.Mater.*, 2011, **23**, 1089–1115.
5 Ian. V. Lightcap and P. V. Kamat, *Acc. Chem. Res.,* 2013**, 46**, 2235–2243.
6 J. f. Wang, Q.F. Cheng and Z. Y. Tang, *Chem. Soc. Rev.*, 2012, **41**, 1111-1129.
7 D. R. Dreyer, S. J. Park, C. W. Bielawski and R. S. Ruoff , *Chem. Soc. Rev.*, 2010,**39**, 228-240.

RSC Advances Accepted Manuscript

8 S. Gadipelli, J. Ford,J. M. Simmons, W. Zhou and T. Yildirim, *Angew. Chem. Int. Ed.*, 2010, **49**, 8902–8904.

9 S. Eiden-Assmann, J. Widoniak, and G. Maret, *Chem. Mater.,* 2004, **16**, 6–11.

10 W. S. Hummers, R. E. Offeman, *J. Am. Chem. Soc.*, 1958, **80**, 1339–1339.

11 L. J. Cote, F. Kim and Jiaxing Huang, *J. Am. Chem. Soc.*, 2009, **131**, 1043–1049.

12 A. V. Talyzin , B. Sundqvist , T. Szabó , I. Dékány and V. Dmitriev, *J. Am. Chem. Soc.*, 2009, **131**, 18445–18449.

13 Z.-M. Wang, K. Hoshinoo, K. Shishibori, H. Kanoh and K. Ooi, *Chem. Mater.*, 2003, **15**, 2926–2935.

14 J. B. Benedict, R. Freindorf, E. Trzop, J. Cogswell, and P. Coppens, *J. Am. Chem. Soc.*, 2010, **132**, 13669–13671.

15 X. H. Cao, B. Zheng, X.H. Rui, W. H. Shi, Q. Y. Yan and H. Zhang, *Angew. Chem. Int. Ed.*, 2014, **53**, 1404–1409.

16 H. G. Yang, C. H. Sun, S. Z. Qiao, J. Zou, G. Liu, S. C. Smith, H. M. Cheng and G. Q. Lu, *Nature*, 2008, **453**, 638–641.

17 G. Jiang, Z. Lin, C. Chen, L. Zhu, Q. Chang, N. Wang, W. Wei and H. Tang, *Carbon*, 2011, **49**, 2693–2701.

18 R. K. Upadhyay, N. Soin and S. S. Roy, *RSC Advances*, 2014, **4**, 3823–3851.

19 H. Xu, P. Reunchan, S. Ouyang, H. Tong, N. Umezawa, T. Kako and J. Ye, *Chem. Mater.,* 2013, **25**, 405–411.

RSC Advances Accepted Manuscript

This journal is © The Royal Society of Chemistry [year]